Electronic properties and magnetism of ruthenium clusters

Deng Kaiming
Department of Applied Physics, Nanjing University of Science and Technology, Nanjing, Jiangsu 210014, People's Republic of China

Yang Jinlong
*International Center for Materials Physics, Academia Sinica, Shenyang 110015, People's Republic of China and Center for Fundamental Physics, University of Science and Technology of China, Hefei, Anhui 230026, People's Republic of China**

Xiao Chuanyun
Chinese Center of Advanced Science and Technology, (World Laboratory), P.O. Box 8730, Beijing 100080, China and Department of Physics, Central China Normal University, Wuhan, Ilubei 430070, People's Republic of China

Wang Kelin
Center for Fundamental Physics, University of Science and Technology of China, Hefei, Anhui 230026, People's Republic of China
(Received 14 November 1995)

The electronic properties and magnetism of Ru_N clusters ($N=4$, 6, 10, 13, 19, 43, and 55) are studied using the discrete-variational local-spin-density-functional method. The bond lengths in the clusters with $N\leqslant 13$ are optimized, and the cluster binding energies are found to increase monotonically with the increase of cluster size. All clusters except Ru_{19} are shown to have magnetic ground states. The average magnetic moments per atom for the Ru_N are found to decrease rapidly with the increase of the cluster size, although small oscillation exists. The calculated moments per atom for Ru_{10} and Ru_{13} clusters are in good agreement with the experimental values. Multiple magnetic solutions are explored, and double magnetic solutions are found for the icosahedral (I_h) Ru_{13} cluster which is used successfully to eliminate the contradiction between the previous theory and experiment on the moment of Ru_{13} cluster. The electronic structures of Ru_N clusters are calculated, and indicate that all clusters are metallic in behavior. The comparison between the Ru_{55} cluster and the bulk counterpart indicates that Ru_{55} has shown bulklike properties in the binding energy, magnetism, valence-bandwidth, and density of states. Based on electronic-structure results, the reactivity of Ru_6, Ru_{19}, and Ru_{43} clusters toward H_2, N_2, and CO molecules is predicted. [S0163-1829(96)10927-9]

I. INTRODUCTION

According to Hund's rules, there exists magnetism in isolated atoms of $3d$, $4d$, and $5d$ transition-metal (TM) elements because all of them have unfilled localized d states. In solids, however, only a few $3d$ (TM's, Fe, Co, and Ni) are found to form ferromagnetic materials. None of the $4d$ or $5d$ solids are magnetic. These elements are, however, characterized by significant spin-orbit coupling, and, if they could be made magnetic, they might provide a class of magnetic materials with enhanced magnetocrystalline anisotropy.[1]

Because of the reduced dimensionality and coordination number as well as enhanced symmetry in both clusters of atoms and monolayer films, it is expected that magnetism would be enhanced in clusters of already ferromagnetic materials, and that magnetization might be found in low-dimensional systems of appropriate bulk nonmagnetic materials, most probably in those of the nonmagnetic TM's.[2,3]

Many theoretical[4–11] and experimental[12–16] studies have been focused on $3d$-TM clusters. For small iron-group clusters (Fe, Co, and Ni), both theories[4–8] and experiments[13,14,16] have shown greater average magnetic moments per atom in the clusters than in the bulk phase, and found that the average moments per atom in these clusters are almost independent of the cluster size. For clusters of nonferromagnetic $3d$ TM's such as V_9, and Cr_9, although theoretical calculations by Pastor, Dorantes-Davila, and Benneman,[7] and Liu, Khanna, and Jena[2] predicted large magnetic moments in both clusters ($2.78\mu_B$ and $3.89\mu_B$ per atom, respectively), experimental measurements[12,15] have so far given almost nonmagnetic results with small upper limits of $0.59\mu_B$ and $0.77\mu_B$ per atom for V_9 and Cr_9 clusters, respectively. There are also conflicting reports on whether V monolayer films are ferromagnetic.[17–19]

Studies on magnetism of $4d$-TM clusters have to date been rather limited.[1,3,20–22] Via local-spin-density (LSD) functional calculations, Reddy, Khanna, and Dunlap predicted that Pd_{13}, Rh_{13}, and Ru_{13} clusters will all be magnetic. The prediction for Rh_{13} cluster was soon confirmed experimentally by Cox *et al.*,[3] who observed that small Rh_N ($N=9$–34) clusters show magnetic ordering with giant moments, and found that the average moments per atom of the Rh_N clusters have a strong dependence on cluster size, which is in contrast to the nearly size-independent behavior of the moments per atom found in iron-group clusters. There is, however, significant quantitative discrepancy between the prediction of Ref. 1 and the measurement of Ref. 3. The average moment per atom of Rh_{13} was measured to be $0.48\mu_B$, which is only one-third the value of $1.62\mu_B$ predicted by Reddy, Khanna, and Dunlap.

Recently, such discrepancies between theories and experiments have been eliminated partially by the finding that both $3d$- and $4d$-TM clusters may have more than one self-consistent magnetic solution at their equilibrium geometries.[23–27] Lee and Callaway[23] studied the possible multiple magnetic solutions in V and Cr clusters with bcc structures, and found that there exist as many as four or five magnetic states in V_9 and Cr_9 clusters for some interatomic spacings. They found that the ground states of the clusters correspond to the lowest-spin solutions with magnetic moments in good agreement with the experimental ones, and that the magnetic states obtained in previous studies are just their highest-spin solutions. At nearly the same time, we studied the possible multiple solutions in small Rh_N ($N=2$–55) clusters,[25–27] and found that there exist three magnetic solutions in an icosahedral (I_h) Rh_{13} cluster at its equilibrium configuration. One of the solutions is the same as that obtained by Reddy, Khanna, and Dunlap,[1] but now it is only a metastable state in our calculations. The magnetic moment of our lowest-spin solution agrees well with the experimental one for Rh_{13} cluster. All of these studies indicate that it is helpful to examine the possibility of multiple magnetic solutions when distinct contradictions appear between theoretical predictions and experimental findings for cluster magnetism.

There are also discrepancies on the magnetic moments of Ru_N clusters between theory and experiment. Reddy, Khanna, and Dunlap[1] proposed that Ru_{13} cluster with I_h and cuboctahedral (O_h) symmetries will be magnetic, and that the magnetic ground state is determined to be the I_h cluster, with a magnetic moment of $12\mu_B$ in total, or $0.92\mu_B$ per atom. Cox *et al.*[3] studied the Ru_{10-115} clusters experimentally, but no magnetic deflection was observed for all of the Ru clusters within the limits of their experimental resolution. Using the superparamagnetic model,[9] they estimated the upper limits of the moments for Ru_{10}, Ru_{13}, and Ru_{115} to be $0.32\mu_B$, $0.29\mu_B$, and $0.09\mu_B$ per atom, respectively. The prediction of Ref. 1 is obviously beyond the experimental uncertainty. Whether Ru_N clusters have magnetism is still an open question. On the other hand, experimental evidence has been revealed recently by Pfandzelter, Steierl, and Ran[21] that Ru monolayer film is ferromagnetic when grown on the C(0001) substrate, which to our knowledge is the first observation reported of the spontaneous $4d$ ferromagnetism in two-dimensional systems.

In this paper, we performed a comprehensive first-principles study on Ru_N clusters with $N=4$, 6, 10, 13, 19, 43, and 55, with the aim to explore the size dependence of the electronic properties and magnetism of ruthenium clusters and the transition to bulk properties. We placed our emphasis on answering the following questions: (a) Do Ru_N clusters have magnetic moments? (b) If so, how do the moments of Ru_N clusters evolve with the cluster size? (c) Do multiple magnetic solutions also exist in Ru_N clusters? (d) If so, can they be used to solve the discrepancy between the previous theory and experiment? (e) How do the cluster properties evolve into the bulk ones? In what follows, we will first describe our theoretical method in Sec. II and then present our results and discussions in Sec. III. Finally a summary is given in Sec. IV.

II. METHOD

The method we employed is the discrete-variational (DV) LSD method. Since it has been described in detail elsewhere,[28,29] we only give a brief description here. The electronic structure of the cluster was determined by solving the Kohn-Sham equations self-consistently. The exchange-correlation potential was taken to be of the spin-dependent von Barth-Hedin form[30] parametrized by Moruzzi, Janak, and Williams.[31] We adopted the self-consistent-charge and frozen-core approximations in this study. The cluster spin orbitals were expanded in terms of numerical atomic basis functions, with the expansion coefficients determined by solving the secular equations iteratively. The numerical atomic basis functions were obtained from local-density-functional (LDF) calculation on the Ru atom having the configuration $4d^7 5s^{0.9} 5p^{0.1}$. The elements of the Hamiltonian and the overlapping matrices were calculated by a weighted summation over a set of grid points according to the Diophantine sampling rules. To reduce the size of the Hamiltonian and the overlapping matrices in block-diagonalized form, the basis was symmetrized in block-diagonalized form according to the irreducible representation of the cluster symmetry group. Sufficient convergence was achieved for both the electronic spectrum and the binding energy by using 1200 sampling points per atom for Ru_4 and Ru_6 and 600 points for the rest of the clusters in our numerical integrations. To explore the possible multiple magnetic solutions, we made spin-unrestricted calculations on the electronic structure for each cluster using input potentials with several different initial spin polarizations, and allowing the system to develop its own magnetic moment as the iterative calculation converges to a self-consistent solution. For cases when there are more than one self-consistent solution, we chose the one with the largest cluster binding energy to be our ground-state solution for the geometrical configuration we have chosen.

III. RESULTS AND DISCUSSIONS

A. Ru_{13}

To better compare our results with previous theoretical studies and with experiment, we first discuss the results for Ru_{13}. We have considered this cluster with three possible high symmetries, i.e., I_h, O_h, and D_{3h}. The geometries of the I_h and O_h Ru_{13} clusters are an icosahedron and a cuboctahedron, respectively. The structure of the D_{3h} Ru_{13} cluster, which is a compact portion of a hcp lattice (bulk Ru is hcp), is obtained from the O_h Ru_{13} cluster by rotating any triad of nearest-neighbor surface atoms by 60° about their center.

For each Ru_{13} cluster, we calculated its binding energy at several internuclear configurations and determined its equilibrium bond length by maximizing the binding energy. The equilibrium bond lengths and corresponding binding energies for Ru_{13} clusters are presented in Table I. From Table I, one can see that the ground state of the Ru_{13} cluster corresponds to the I_h geometry, which is more stable than the O_h and D_{3h} geometries by 0.40 and 0.26 eV, respectively. Compared with the results of Ref. 1, the bond lengths optimized for the I_h and O_h clusters in the two calculations are almost the same, but the binding energies have large differences. We believe that the smaller binding energies of Ref. 1 result from their choice of smaller basis set ($4d^7 5s^1$).

TABLE I. The equilibrium bond lengths (r_e), binding energies (E_b) per atom, and magnetic moments for the Ru_N clusters. For Ru_{13}, r_e is the radial bond length between the central and surface atoms. Values in parentheses correspond to metastable minimum.

Cluster	Symmetry	r_e (a.u.)	E_b (eV/atom)	Magnetic moment (μ_B)
Ru_4	T_d	4.65	3.67	4
Ru_6	O_h	4.81	4.57	6
Ru_{10}	D_{4d}	4.86	5.05	4
Ru_{13}	I_h	4.80	5.23	4
		(4.80	5.21	12)
	O_h	4.90	5.20	14
		(4.90	5.17	18)
	D_{3h}	4.90	5.21	8
		(4.90	5.16	12)
Ru_{19}	D_{5h}	5.06[a]	5.78	0
	O_h	(5.06[a]	5.66	4)
		5.06[a]	5.66	8
		(5.06[a]	5.66	12)
Ru_{43}	I_h	(5.06[a]	6.13	0)
		5.06[a]	6.15	24
	O_h	5.06[a]	6.17	6
Ru_{55}	I_h	5.06[a]	6.45	12
	O_h	5.06[a]	6.56	6

[a]Not optimized; taken to be the average value of the bulk hcp lattice.

With the equilibrium bond lengths obtained above, we further calculated the electronic structures of Ru_{13} clusters. The main results can be found in Tables I–IV. Here we will focus on discussing the results of the magnetic moments only, leaving the rest of the results to be discussed together with other clusters in Sec. III B. Table I lists the total magnetic moments of all the Ru_{13} clusters at their equilibrium configurations. From this table, one finds that all of the I_h, O_h, and D_{3h} Ru_{13} clusters have magnetic ground states with total moments of $4\mu_B$, $14\mu_B$, and $8\mu_B$, respectively. Many calculations[8,24] on 13-atom clusters of the iron-group atoms occupying equivalent volumes have shown that, for a given cluster over a wide range of interatomic spacings including the equilibrium separation, the higher the order of the cluster symmetry group is, the higher the magnetic moment will be. As seen above, this rule no longer works for $4d$ Ru_{13}. A similar anomaly in the symmetry-moment relationship was found by us for $4d$ Ru_{13} (I_h, O_h, and D_{3h}).[25] The moment per atom we obtained for the I_h Ru_{13} cluster is $0.31\mu_B$, which is much smaller than the one obtained by Reddy, Khanna, and Dunlap,[1] but in good agreement with the experimental upper limit of $0.29\mu_B$. As will be shown next, these results can be understood in terms of the multiple magnetic solutions.

As is well known, in the LDF formulation, the exchange-correlation potential in the Kohn-Sham equations is a function of the charge density of the system. The solution to the Kohn-Sham equations is then obtained by optimizing the charge distribution of the system only, which will lead to just one self-consistent solution to the system. In the LSD scheme, however, the exchange-correlation potential depends not only on the charge distribution but also on the spin polarization of the system. Therefore, the Kohn-Sham equations should be solved by simultaneously optimizing the charge and spin distributions of the system, and this can

TABLE II. The data of the ground-state electronic structure for the Ru_N clusters (eV).

Cluster	Symmetry	HOMO	LUMO	E_F	VBW
Ru_4	T_d	−4.75	−4.75	−4.75	5.59
Ru_6	O_h	−4.31	−4.31	−4.31	6.76
Ru_{10}	D_{4d}	−4.91	−4.85	−4.88	6.67
Ru_{13}	I_h	−5.34	−5.34	−5.34	7.24
Ru_{19}	D_{5h}	−6.38	−6.28	−6.33	7.68
Ru_{43}	O_h	−6.07	−6.07	−6.07	7.21
Ru_{55}	O_h	−6.78	−6.74	−6.76	7.70

TABLE III. The ground-state electronic configurations for the Ru_N clusters.

	HOMO		
Cluster	Symbol	Electrons	Electronic configuration
Ru_4	$e\downarrow$	1	open
Ru_6	$e_u\downarrow$	1	open
Ru_{10}	$e_1\uparrow$	2	closed
Ru_{13}	$h_u\uparrow$	4	open
Ru_{19}	$e_2''\downarrow$	2	closed
Ru_{43}	$t_{2u}\uparrow$	1	open
Ru_{55}	$t_{2u}\uparrow$	3	closed

TABLE IV. Mulliken orbital and spin populations for the ground-state configurations of Ru_N clusters, a, b, c, d, and e are the types of inequivalent atoms within the cluster point group, and the number of atoms for each inequivalent type is given in parentheses.

		Charge			Net spin			
		$4d$	$5s$	$5p$	$4d$	$5s$	$5p$	total
Ru_4		7.23	0.60	0.17	1.03	−0.02	−0.01	1.00
Ru_6		7.28	0.52	0.20	1.01	−0.01	0.00	1.00
Ru_{10}	$a(8)$	7.26	0.50	0.26	0.48	0.01	0.01	0.50
	$b(2)$	7.28	0.52	0.09	0.33	−0.02	−0.01	0.00
Ru_{13}	$a(1)$	7.31	0.46	0.46	−0.10	−0.01	0.03	−0.08
	$b(12)$	7.25	0.47	0.26	0.35	−0.01	0.00	0.34
Ru_{19}	$a(2)$	7.27	0.48	0.25	0.00	0.00	0.00	0.00
	$b(2)$	7.35	0.49	0.00	0.00	0.00	0.00	0.00
	$c(5)$	7.20	0.60	0.45	0.00	0.00	0.00	0.00
	$d(10)$	7.20	0.49	0.22	0.00	0.00	0.00	0.00
Ru_{43}	$a(1)$	6.88	0.44	1.02	−0.10	0.00	−0.01	−0.11
	$b(12)$	7.07	0.29	0.89	0.05	0.00	0.00	0.05
	$c(6)$	7.07	0.55	0.71	−0.06	−0.01	0.01	−0.06
	$d(24)$	7.14	0.42	0.22	0.24	0.00	0.00	0.24
Ru_{55}	$a(1)$	7.08	0.63	1.09	−0.06	0.00	0.08	0.02
	$b(12)$	7.17	0.29	0.52	0.05	0.00	0.00	0.05
	$c(6)$	7.07	0.65	0.48	0.01	0.00	0.00	0.01
	$d(24)$	7.11	0.53	0.39	0.12	0.01	0.00	0.13
	$e(12)$	7.12	0.45	0.24	0.19	0.00	0.00	0.19

yield more than one solution. These solutions correspond to the local minima of the total energy as a function of the magnetic moment of the system, among which the one that gives the lowest total energy is regarded as the ground state of the system, and the rest, with higher energies, are only metastable states. In other words, different choices of the input potentials in the LSD calculations may lead to different self-consistent magnetic solutions. In fact, in both $3d$-TM solids[32,33] and $3d$- and $4d$-TM clusters,[8,23–27] multiple magnetic solutions have been found. As seen in Table I, we found that all of the Ru_{13} clusters have two self-consistent magnetic solutions at their equilibrium configurations, which we referred to as the low- and high-spin solutions, respectively. For all Ru_{13} clusters, the low-spin states have lower energies than the high-spin ones, and hence correspond to the ground states. For the I_h Ru_{13} cluster, our low-spin solution can satisfactorily explain the experimental measurement on the cluster moment, as has been described above, while our high-spin solution is just the same as the only solution obtained by Reddy, Khanna, and Dunlap.[1] So, we can conclude that the discrepancy between the experiment and previous theory about the magnetism of the Ru_{13} cluster arises from the fact that the previous theory found only a metastable magnetic solution for the cluster.

The local magnetic moments of the I_h Ru_{13} cluster at its equilibrium configuration are given in Table IV. One finds that each of the surface atoms has a larger moment than the central one. This results consistency with those found in iron-group clusters. It is worthwhile to mention that magnetic interactions between the central and surface atoms are antiferromagnetic in I_h Ru_{13}. A similar antialignment has also been found in the Fe_{13} cluster,[34] the element immediately above Ru in the Periodic Table.

B. Ru_N (N=4, 6, 10, 19, 43, and 55)

Since the structures of clusters still cannot be determined experimentally, we assumed one probable geometry for each of the Ru_4, Ru_6, and Ru_{10} clusters, and optimized their bond lengths by maximizing the calculated binding energies within the symmetry constraints. For Ru_{19}, Ru_{43}, and Ru_{55}, we made studies in both the icosahedral (D_{5h} and I_h) and cuboctahedral (O_h) growth sequences, with the bond length (5.06 a.u.) taken to be the average value in the hcp lattice of bulk Ru. The geometries we chose for these clusters are (a) T_d Ru_4, tetrahedron; (b) O_h Ru_6, octahedron; (c) D_{4d} Ru_{10}, twisted double square pyramid; (d) D_{5h} Ru_{19}, double icosahedron; (e) O_h Ru_{19}, Ru_{43}, and Ru_{55}, all taken from parts of fcc lattice; and (f) I_h Ru_{43} and Ru_{55}, icosahedron. Details of our structural models can be found in Ref. 26.

The equilibrium properties for the Ru_N clusters are presented in Table I. Compared with the bulk interatomic spacing of 5.06 a.u., one may find small bond-length contractions in all of the optimized Ru clusters. The contraction ratio ranges from 3% in $Ru_{13}(O_h)$ to 8% in $Ru_4(T_d)$. Such a contraction effect has been found in many metal clusters both theoretically[8,24–27,34] and experimentally,[35] and can be considered as a reflection of cluster surface effects.

Table I also lists the binding energies for the Ru_N clusters. Compared with the corresponding fcc-like geometry, the icosahedral-like geometry has lower energies for both the Ru_{13} and Ru_{19} clusters, and hence corresponds to the ground state, while it has higher energies for the Ru_{43} and Ru_{55} clusters. The ground states of the latter two are thus both O_h clusters. Therefore, we may suggest, from the energy point of view, that the transition between the icosahedral and the cuboctahedral growths occur for $N \leqslant 43$. Of course, we must be cautious in drawing such a conclusion from our results, since the binding energies of the Ru_{19}, Ru_{43}, and Ru_{55} clusters have been calculated with an unoptimized geometry.

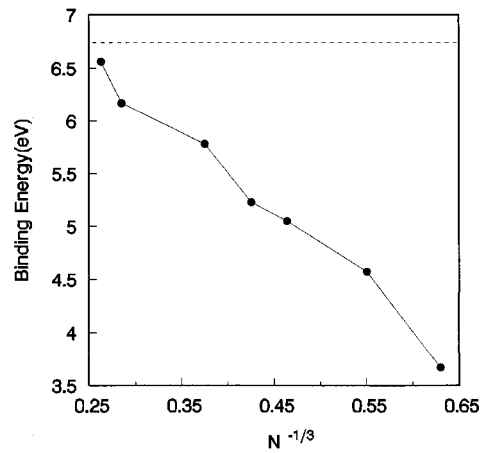

FIG. 1. Size dependence of the binding energies per atom for Ru_N clusters at ground-state geometrical configurations. The dashed line corresponds to the bulk cohesive energy.

Figure 1 shows the size dependence of the binding energies per atom for all Ru_N clusters at ground-state configurations. We see that all clusters have a binding energy per atom smaller than the bulk cohesive energy (6.74 eV). The cluster binding energy increases monotonically with the increase of the cluster size, and reaches a value of 6.56 eV at the Ru_{55} cluster, which is very close to the bulk value with a difference of no more than 3%.

The total magnetic moments for all Ru_N clusters are obtained from Mulliken spin population analysis, and are given in Table I. From this table, one may find that all clusters except Ru_{19} have magnetic ground states. The average magnetic moments per atom for Ru_N clusters at the ground-state configurations are shown in Fig. 2 as a function of the cluster

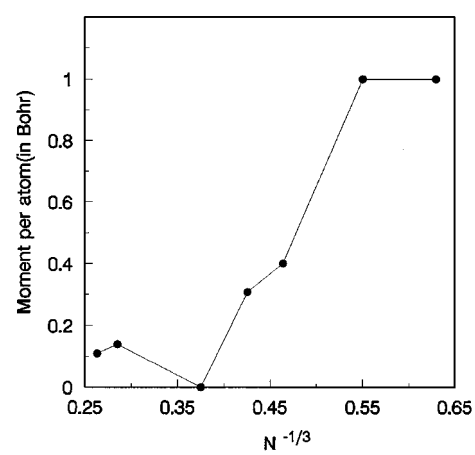

FIG. 2. Size dependence of the magnetic moments per atom for Ru_N clusters at ground-state geometrical configurations.

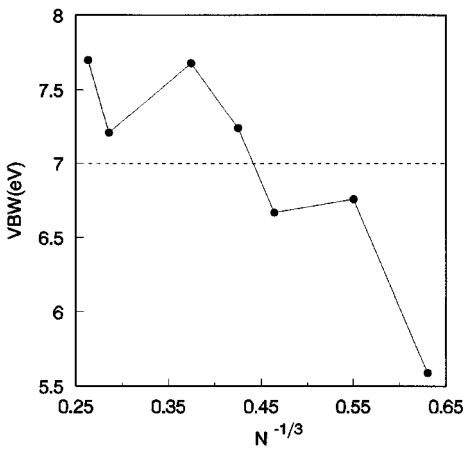

FIG. 3. Size dependence of the valence-band-width (VBW) for Ru_N clusters at ground-state geometrical configurations. The dashed line corresponds to the bulk VBW.

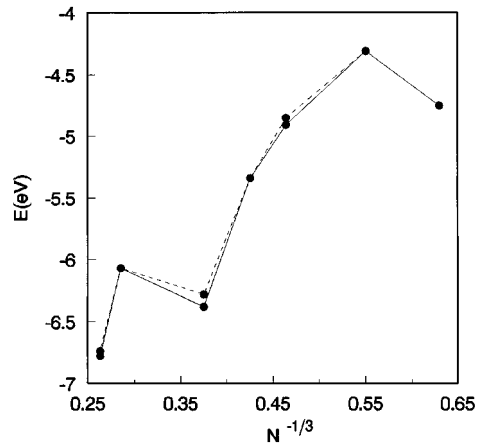

FIG. 4. Size dependence of the HOMO (solid curve) and LUMO (dashed curve) for Ru_N clusters at ground-state geometrical configurations.

size. From this figure, we see that the average magnetic moment per atom in Ru_N clusters decreases rapidly with the increase of N, although small oscillation does exist. This feature is both different from the behavior in Rh_N clusters,[3,26] where the oscillation is much more significant, and is in contrast to the nearly size-independent behavior in iron-group clusters. The moments we obtained for the Ru_{10} and Ru_{13} clusters are both $4\mu_B$, or $0.40\mu_B$ and $0.31\mu_B$ pre atom, respectively. They are in good agreement with the experimental upper limits[3] of $0.32\mu_B$ and $0.29\mu_B$, respectively. The moment for the Ru_{55} cluster is calculated to be $6\mu_B$, or $0.11\mu_B$ per atom, which has reached such a depressed value as to be well comparable with the experimental upper limit of $0.09\mu_B$ for Ru_{115}.

We have explored multiple magnetic solutions for all Ru_N clusters, and obtained the following results: (a) for all Ru_N clusters at the ground-state geometrical configurations, only the I_h Ru_{13} cluster is found to have more than one magnetic state, and there exists only the paramagnetic solution for D_{5h} Ru_{19}; and (b) for clusters with structures other than the ground-state geometries, O_h and D_{3h} Ru_{13} both have two magnetic solutions, O_h Ru_{19} has three magnetic solutions, and I_h Ru_{43} has a magnetic and a paramagnetic solutions. It is worthwhile to point out that both I_h and O_h Ru_{55} clusters have only one magnetic solution, although the energy parameters ΔE for them, which we proposed in studies on Rh_N clusters[25,26] as criteria to judge the possibility of multiple magnetic solutions, are both very small (0.06 and 0.04 eV, respectively).

The data for the ground-state electronic structure of the Ru_N clusters are listed in Table II and shown in Figs. 3 and 4. From Table II and Fig. 3, we see that the valence-band-width (VBW) changes with the cluster size in a somewhat complex way. Two local minima occur at Ru_{10} and Ru_{43}, and the VBW reaches its largest values at Ru_{13} and Ru_{55}. It is worth noting that the VBW exceeds the bulk value of about 7.0 eV for Ru_N clusters with $N \geqslant 19$. This is very different from the case in Rh clusters, where VBW's for all Rh_N ($N=2$–55) clusters are smaller than the bulk value.[25–27] The HOMO (highest occupied molecular orbital) and LUMO (lowest unoccupied molecular orbital) as functions of the cluster size are shown in Fig. 4. The gap between the HOMO and LUMO is found to be rather small for all clusters, indicating that the clusters are metallic in behavior. Both the HOMO and LUMO have two local maxima, i.e., at Ru_6 and Ru_{43}, respectively, and a local minima at Ru_{19}. Since Ru is known to be important in catalysis, it is interesting to link the variation of the HOMO with the cluster size to the reactivity of Ru_N clusters toward H_2, N_2 and CO molecules. Following the method of Rosen and Rantala,[6] we predict that Ru_6 and Ru_{43} might have substantial reactivity, while Ru_{19} would show remarkable stability toward H_2, N_2, and CO molecules.

For a cluster, the number of electrons in the HOMO determines its ground-state electronic configuration. From Table III, we see that the HOMO is occupied by minority-spin electrons for Ru_4, Ru_6, Ru_{19}, and Ru_{55}, and by majority-spin electrons for Ru_{10}, Ru_{13}, and Ru_{43}. This picture is very different from that obtained for $3d$ ferromagnetic clusters, where the HOMO is always occupied by the minority-spin electrons.[5,6,36] The HOMO's of the Ru_{10}, Ru_{19}, and Ru_{55} clusters are fully occupied, which leads to ground states with closed electronic shells. Thus these clusters are expected to show remarkable stability. The HOMO's of the Ru_4, Ru_6, Ru_{13}, and Ru_{43} clusters are partially occupied; therefore, these clusters have degenerate ground states. According to the Jahn-Teller theorem, these clusters tend to distort further toward lower symmetry so as to lift the degeneracy of their ground states and lower their energies. It should be pointed out, however, that the distorted cluster may also increase its energy if it possesses a reduced spin. Accordingly, it depends on a compromise between two such effects whether or to what extent the Jahn-Teller distortion may take place. It is well known in atomic physics that an atom with a closed electronic shell will show chemical inertness and high stability, while the adjacent atoms with open electronic shells will be chemically reactive. For a cluster, the chemical reactivity depends not only on its electronic structure but also on its geometry.[37] Supposing that the electronic structure is the dominant factor for the cluster reactivity, one would come to the conclusion that Ru_{19} will be

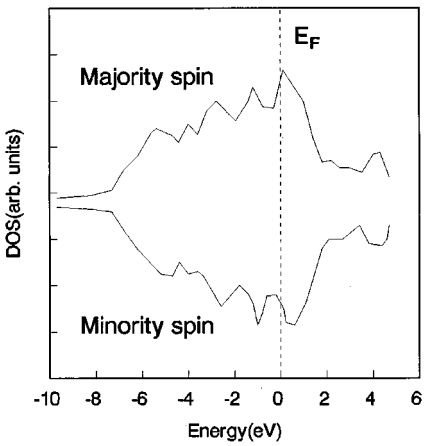

FIG. 5. Density of states for the O_h Ru_{55} cluster.

chemically inert while Ru_6 and Ru_{43} will be reactive, in support of the reactivity analysis above following Rosen and Rantala.[6]

The Mulliken orbital and spin populations for the Ru_N clusters are given in Table IV. With reference to the atomic configuration $4d^7 5s^1 5p^0$, we see that there is charge transfer from $5s$ to $4d$ and $5p$ orbitals in all clusters. The magnetic interactions are found to be antiferromagnetic between adjacent shells of atoms in both Ru_{13} and Ru_{43} clusters, while they are ferromagnetic in all other clusters except Ru_{19}, where the interactions between atoms are paramagnetic.

To examine how cluster properties evolve into bulk ones, we make a comparison of the density of states (DOS) for Ru_{55} cluster with the bulk DOS. Figure 5 shows the DOS for majority- and minority-spin states for this cluster at its ground-state geometrical configuration (O_h), which is obtained by broadening the discrete one-electron energy levels of the cluster with a Lorentzian function of fixed half-width 0.2 eV and a summation over them. From this figure, one can see that there are four peaks below the Fermi level, which are in one-to-one correspondence with the four peaks in bulk DOS obtained by band-structure calculation on a fcc lattice.[31] The exchange splitting is observed to be very small, in agreement with the small magnetic moment for this cluster. The VBW of the Ru_{55} is calculated to be 7.70 eV, in close agreement with the bulk value[31] of about 7.0 eV. From the comparison of properties made above between the Ru_{55} cluster and the bulk counterpart in the binding energy, magnetic moment, valence-band-width, and DOS, we can say that Ru_{55} cluster has already shown bulklike properties.

Finally, we discuss the temperature dependence of the magnetism in the Ru_N clusters. Stern-Gerlach experiments on small TM clusters have shown an abnormal temperature dependence in certain clusters: the magnetization increases with temperature.[13] Recently, Reuse, Khanna, and Berne[38] explored this abnormal behavior by performing LSD calculations for the Ni_{13} cluster with various fixed-spin configurations. They found that there exist a number of higher-spin states close to the ground state in the Ni_{13} cluster and suggested that this might be responsible for the abnormal temperature dependence of magnetization in certain TM clusters. We believe that multiple magnetic solutions of clusters could provide an alternative insight into this problem. For example, the I_h Ru_{13} cluster has double magnetic states, with the low-spin one being the ground state (see Table I). Since the high-spin state lies close to the low-spin one, it is clear that if an ensemle of the Ru_{13} clusters are heated, some of them would occupy the high-spin state. This would lead to an increase in the cluster magnetization, which is determined by the overall cluster moment, if the occupation of the high-spin state overrides the decrease in magnetization due to an increase in temperature. In addition, since the O_h and D_{3h} geometries are slightly higher in energy than the I_h geometry for the Ru_{13} cluster, considerable O_h and D_{3h} isomers in addition to I_h ones may also be produced at higher temperature. Since the O_h and D_{3h} isomers both have larger magnetic moments than the I_h ones, they contribute to enhancing the cluster magnetization. From the above two aspects of the analyses, we could predict that the Ru_{13} cluster would reveal an enhanced magnetization as the temperature increases. A similar analysis can be applied to other clusters.

IV. SUMMARY

In this paper, we have reported a comprehensive study of the electronic properties and magnetism of Ru_N clusters using the first-principles DV-LSD method. The results we have obtained can be summarized as follows.

(1) There are bond-length contractions in all optimized Ru clusters. The value of the contraction is about 3–8% as compared with the bulk interatomic spacing. The binding energies of the clusters are all smaller than the bulk cohesive energy (6.74 eV), and show a monotonic growth with the increase of the cluster size.

(2) Based on the studies of the binding energy for the icosahedral-like and fcc-like Ru_{13}, Ru_{19}, Ru_{43}, and Ru_{55} clusters, we suggest that the transition between the icosahedral and the cuboctahedral growths of Ru_N clusters occurs at $N \leqslant 43$.

(3) All clusters except Ru_{19} are found to have magnetic ground states. The calculated average moments per atom for the Ru_{10}, Ru_{13}, and Ru_{55} clusters are $0.40\mu_B$, $0.31\mu_B$, and $0.11\mu_B$, respectively. They are in good agreement with the experimental ones ($Ru_{10}<0.32\mu_B$, $Ru_{13}<0.29\mu_B$, and $Ru_{115}<0.09\mu_B$, respectively). The average magnetic moments per atom of the Ru_N clusters are found to decrease rapidly with the increase of the cluster size, although a small oscillation exists.

(4) The multiple magnetic solutions are explored for all of the clusters. Only the Ru_{13} cluster is found to posses more than one magnetic state at the ground-state geometrical configuration (I_h cluster), and this has been used successfully to solve the discrepancy between the previous theory and experiment. The multiple magnetic solutions for clusters of other less stable geometries are also explored.

(5) The electronic properties of the Ru_N clusters are calculated. All clusters are found to be metallic in behavior. The Ru_{10}, Ru_{19}, and Ru_{55} clusters have closed electronic shells and thus will be remarkably stable. The Ru_4, Ru_6, Ru_{13}, and Ru_{43} clusters have open electronic shells, so they tend to distort further according to the Jahn-Teller theorem.

(6) The reactivity of Ru_6, Ru_{19}, and Ru_{43} clusters toward H_2, N_2, and CO molecules is predicted. Ru_6 and Ru_{43} are expected to have substantial reactivity, while Ru_{19} will show remarkable stability.

(7) The comparison between the Ru_{55} cluster and its bulk counterpart indicates that Ru_{55} has shown bulklike properties in the binding energy, magnetism, valence-band-width, and density of states.

ACKNOWLEDGMENTS

This work was supported by the National Natural Science Foundation of China and by the Foundations of the Chinese Academy of Science and the National Education Commission for the Returned Chinese Scholars. One of us (Y.J.) gratefully acknowledges the financial support of the Solid Cluster Laboratory of USTC.

*Mailing address.

[1] B. V. Reddy, S. N. Khanna, and B. I. Dunlap, Phys. Rev. Lett. **70**, 3323 (1993).
[2] F. Liu, S. N. Khanna, and P. Jena, Phys. Rev. B **43**, 8179 (1991).
[3] A. J. Cox, J. G. Louderback, S. E. Apsel, and L. A. Bloomfield, Phys. Rev. B **49**, 12 295 (1994).
[4] D. R. Salahub and R. P. Messiuer, Surf. Sci. **106**, 415 (1981).
[5] K. Lee, J. Callaway, and S. Dhar, Phys. Rev. B **30**, 1724 (1985).
[6] A. Rosen and T. T. Rautala, Z. Phys. D **3**, 205 (1986).
[7] G. M. Pastor, J. Dorantes-Davila, and K. H. Benneman, Phys. Rev. B **40**, 7642 (1989).
[8] B. I. Dunlap, Phys. Rev. A **41**, 5691 (1990).
[9] S. N. Khanna and S. Linderoth, Phys. Rev. Lett. **67**, 742 (1991).
[10] Z. Q. Li and B. L. Gu, Phys. Rev. B **47**, 13 611 (1993).
[11] K. Lee and J. Callaway, Phys. Rev. B **48**, 15 358 (1993).
[12] D. M. Cox, D. J. Trevor, R. L. Whetten, E. A. Rohlfing, and A. Kaldor, J. Chem. Phys. **84**, 4651 (1986).
[13] W. A. deHeer, P. Milani, and A. Chatelain, Phys. Rev. Lett. **65**, 488 (1990).
[14] J. P. Bucher, D. C. Douglass, and L. A. Bloomfield, Phys. Rev. Lett. **66**, 3052 (1991).
[15] D. C. Douglass, J. P. Bucher, and L. A. Bloomfield, Phys. Rev. B **45**, 6341 (1992).
[16] J. G. Louderback, A. J. Cox, J. J. Lising, D. C. Douglass, L. A. Bloomfield, Z. Phys. D **26**, 301 (1993).
[17] R. L. Fink, C. A. Ballentine, J. L. Erskine, and J. A. Araya-Pochet, Phys. Rev. B. **41**, 10 175 (1982).
[18] M. Stampanoni, Appl. Phys. A **49**, 449 (1989).
[19] S. Lin and S. D. Bader, Phys. Rev. B **44**, 12 062 (1991).
[20] L. Goodwin and D. Salahub, Phys. Rev. A **47**, R774 (1993).
[21] R. Pfandzelter, G. Steierl, and C. Ran, Phys. Rev. Lett. **74**, 3467 (1995).
[22] G. R. Harp, S. S. P. Parkin, W. L. O'Brien, and B. P. Tonner, Phys. Rev. B **51**, 12 037 (1995).
[23] K. Lee and J. Callaway, Phys. Rev. B **49**, 13 906 (1994).
[24] K. Minra, H. Kimura, and S. Imanaga, Phys. Rev. B **50**, 10 335 (1994).
[25] Yang Jinlong, F. Toigo, Wang Kelin, and Zhang Manhong, Phys. Rev. B **50**, 7173 (1994).
[26] Yang Jinlong, F. Toigo, and Wang Kelin, Phys. Rev. B **50**, 7915 (1994).
[27] Yang Jinlong, F. Toigo, and Wang Kelin (unpublished).
[28] B. Delley and D. E. Ellis, J. Chem. Phys. **76**, 1949 (1982).
[29] B. Delley, D. E. Ellis, A. J. Freeman, E. J. Baerends, and D. Post, Phys. Rev. B **27**, 2132 (1983).
[30] U. von Barth and L. Hedin, J. Phys. C **5**, 1629 (1972).
[31] V. L. Moruzzi, J. F. Janak, and A. R. Williams, *Calculated Electronic Properties of Metals* (Pergamon, New York, 1978).
[32] V. Moruzzi, P. Marcus, and P. C. Pattnaik, Phys. Rev. B **37**, 8003 (1988).
[33] V. Moruzzi, Phys. Rev. Lett. **57**, 2211 (1986).
[34] B. I. Dunlap, Z. Phys. D **19**, 255 (1991).
[35] G. Apai, J. F. Hamilton, J. Stohr, and A. Thompson, Phys. Rev. Lett. **43**, 165 (1979).
[36] Yang Jinlong, Xiao Chuanyun, Xia Shangda, and Wang Kelin, Phys. Rev. B **48**, 12 155 (1993).
[37] S. N. Khanna and P. Jena, Phys. Rev. B **51**, 13 075 (1995).
[38] F. R. Reuse, S. N. Khanna, and S. Bernel, Phys. Rev. B **52**, R11 650 (1995).